IOPscience iopscience.iop.org

Home Search Collections Journals About Contact us My IOPscience

Persistency properties of models of polymers on simple cubic and face-centred cubic lattices

This article has been downloaded from IOPscience. Please scroll down to see the full text article.

1989 J. Phys. A: Math. Gen. 22 3081

(http://iopscience.iop.org/0305-4470/22/15/022)

View the table of contents for this issue, or go to the journal homepage for more

Download details:
IP Address: 129.252.86.83
The article was downloaded on 01/06/2010 at 06:58

Please note that terms and conditions apply.

J. Phys. A: Math. Gen. **22** (1989) 3081–3093. Printed in the UK

Persistency properties of models of polymers on simple cubic and face-centred cubic lattices

D E Burnette and H A Lim

Supercomputer Computations Research Institute, Florida State University, Tallahassee, FL 32306-4052, USA

Received 4 January 1989, in final form 11 April 1989

Abstract. The first four odd moments of the persistence lengths of trails and silhouettes are studied on two different 3D lattices, the simple cubic lattice and the face-centred cubic lattice. Variations of the averaged persistence lengths with chain lengths (l) and inverse temperatures (θ) are systematically examined. It is found that the averaged persistence lengths scale with a scaling law of the form $\langle X_l^{2k+1}(\theta)\rangle \sim l^{pk\nu(\theta)} f(l)$ where ν is the correlation exponent, p is a parameter, $k = 0, 1, 2, \ldots$ and $f(l) \sim$ constant, in contrast to the results in 2D where $f(l) \sim \log_e l$.

1. Introduction

Recently, there has been some interest in the studies of persistencies of polymeric models [1–5]. This concept is important in many disciplines, especially those in which walks on lattices are used to model the physical systems of interest. For instance, one talks about the persistence lengths in gel electrophoresis of DNA [6] or fragments of DNA in aqueous solutions form lyotropic polymer liquid crystal phases [7].

In the preceding paper [1], we study the first four odd moments of persistence lengths of trails and silhouettes on two-dimensional square and triangular lattices. In particular, the temperature dependence is introduced via the conjugate fugacity factor $e^{I\theta}$, where I is the number of intersections, $\theta = -|\varepsilon|/k_B T$ and $|\varepsilon|$ is the attractive energy of intersection. These models are interesting in the sense that they interpolate between the usual random walk model (RW) and the self-avoiding walk model (SAW) of polymers, and that they model polymers with fused loops [8–16].

In this paper, we shall pursue a parallel study of the persistency properties of these polymeric models on a loose-packed three-dimensional (3D) simple cubic lattice and on a close-packed 3D face-centred cubic lattice. In §2 we shall recall some of the thermodynamical definitions, which we will use in the subsequent sections. Section 3 gives the results of exact enumeration and §§4–6 are devoted to analyses of the data of the simple cubic lattice and the faced-centred cubic lattice. Comparisons and conclusion are presented in §7.

2. Symbols and thermodynamic functions

We recall that if $C(l, I, r)$ denotes the total number of trails (silhouettes) of chain length l, number of intersections I and end-to-end distance r, then for a fixed chain length,

0305-4470/89/153081+13$02.50 © 1989 IOP Publishing Ltd

the total number of trails (silhouettes) and the partition function on a lattice are given, respectively, as [12–15]

$$c(l, I) = \sum_{r} C(l, I, r) \tag{1a}$$

$$Z_l(\theta) = \sum_{I \geq 0} c(l, I) e^{I\theta}. \tag{1b}$$

The $c(l, I)$ tables have been published elsewhere [13–15] and will not be reproduced here. The averaged mth moment of the persistence lengths along the direction of the initial step $(+x)$ is defined by [1, 15]:

$$\langle X_l^m(\theta) \rangle = \frac{\sum_I \sum_r x^m(l, I, r) C(l, I, r) e^{I\theta}}{Z_l(\theta)} \tag{2}$$

where we have used $\hat{x}$ as the generic notation for the direction of the first step, and x is the projected displacement in the $\hat{x}$ direction.

3. Exact enumeration

In our enumeration process, the first step is always fixed along a certain direction to induce the 'initial perturbation' and to reduce the enumeration time by a factor of q, where q is the coordination number of the lattice [1, 15]. We have enumerated the first four odd moments $X^{2k+1}(l, I)$ with $k = 0, 1, 2, 3$ of trails and silhouettes, categorised according to the number of intersections I, and the chain lengths l. A noteworthy point is that since there is in general no topological relation relating the number of trails to the number of their corresponding silhouettes, we have to classify the silhouette configurations by brute force. The computer time required for the classification renders enumerations to high orders impractical. All the enumerations (on the simple cubic lattice and on the face-centred cubic lattice) take about a total of 75 CPU hours on a VAX 8700.

3.1. Simple cubic lattice

The enumeration on this lattice is quite straightforward since the primitive axes are all mutually perpendicular. The basis vectors are the $\hat{x}$, $\hat{y}$ and $\hat{z}$ axes. The enumeration is performed with the first monomeric site rooted at the origin and the first step fixed along $\hat{x}$. It is then easy to see that there are only two sets of topologically distinct configurations [13, 14]:

(i) the second step is along $\hat{x}$;
(ii) the second step is either along $\pm\hat{y}$ or along $\pm\hat{z}$.

We emphasise that overlap of bonds is forbidden. The projected displacement of a configuration is then just the x component of the end-to-end vector of the configuration. Table 1 presents the first three odd moments of the persistence lengths for trails of chain lengths up to $l = 15$ and a maximum number of intersections $I = 5$ on the simple cubic lattice. Table 2 gives the corresponding table for silhouettes.

Table 1. Trails on a simple cubic lattice: (*a*) the first odd moment of the persistence length $X(l, I)$; (*b*) the second odd moment of the persistence length $X^3(l, I)$; (*c*) the third odd moment of the persistence length $X^5(l, I)$.

l	$I = 0$	$I = 1$	$I = 2$	$I = 3$	$I = 4$	$I = 5$
(*a*)	$X(l, I)$					
3	0.31000E2					
4	0.15600E3	0.00000E0				
5	0.76500E3	0.12000E2				
6	0.37340E4	0.12800E3				
7	0.18015E5	0.10680E4	0.12000E2			
8	0.86800E5	0.72480E4	0.20800E3			
9	0.41559E6	0.46068E5	0.21800E4			
10	0.19887E7	0.27318E6	0.18672E5	0.20800E3		
11	0.94787E7	0.15702E7	0.13879E6	0.45120E4		
12	0.45166E8	0.87349E7	0.94661E6	0.48224E5	0.44800E3	
13	0.21463E9	0.47701E8	0.60922E7	0.43521E6	0.91920E4	
14	0.10198E10	0.25568E9	0.37466E8	0.33614E7	0.12874E6	0.35200E3
15	0.48360E10	0.13537E10	0.22345E9	0.24121E8	0.13536E7	0.12896E5
(*b*)	$X^3(l, I)$					
3	0.10300E3					
4	0.74400E3	0.00000E0				
5	0.48690E4	0.12000E2				
6	0.29936E5	0.24800E3				
7	0.17620E6	0.32280E4	0.12000E2			
8	0.10049E7	0.31392E5	0.49600E3			
9	0.55945E7	0.26231E6	0.67400E4			
10	0.30563E8	0.19712E7	0.74184E5	0.20800E3		
11	0.16444E9	0.13784E8	0.68734E6	0.95520E4		
12	0.87375E9	0.91276E8	0.57415E7	0.15094E6	0.44800E3	
13	0.45942E10	0.57999E9	0.44288E8	0.17536E7	0.23784E5	
14	0.23943E11	0.35661E10	0.32173E9	0.17011E8	0.42509E6	0.14080E4
15	0.12383E12	0.21352E11	0.22282E10	0.14718E9	0.54462E7	0.36128E5
(*c*)	$X^5(l, I)$					
3	0.51100E3					
4	0.52560E4	0.00000E0				
5	0.45405E5	0.12000E2				
6	0.35074E6	0.72800E3				
7	0.25069E7	0.15228E5	0.12000E2			
8	0.16922E8	0.21053E6	0.16480E4			
9	0.10934E9	0.23066E7	0.35060E5			
10	0.68242E9	0.21737E8	0.50551E6	0.20800E3		
11	0.41418E10	0.18424E9	0.58561E7	0.29712E5		
12	0.24565E11	0.14436E10	0.59065E8	0.72406E6	0.44800E3	
13	0.14290E12	0.10646E11	0.53865E9	0.11443E8	0.82152E5	
14	0.81766E12	0.74828E11	0.45504E10	0.14098E9	0.22614E7	0.56320E4
15	0.46128E13	0.50578E12	0.36167E11	0.14884E10	0.36580E8	0.21354E6

3.2. Face-centred cubic lattice

The enumeration on this lattice is a little more involved because the axes are not mutually orthogonal. However symmetry factors can be used in our favour. The basis

Table 2. Silhouettes on a simple cubic lattice: (*a*) the first odd moment of the persistence length $X(l, I)$; (*b*) the second odd moment of the persistence length $X^3(l, I)$; (*c*) the third odd moment of the persistence length $X^5(l, I)$.

l	$I=0$	$I=1$	$I=2$	$I=3$	$I=4$	$I=5$
(*a*)	$X(l, I)$					
3	0.31000E2					
4	0.15600E3	0.00000E0				
5	0.76500E3	0.60000E1				
6	0.37340E4	0.64000E2				
7	0.18015E5	0.53400E3	0.20000E1			
8	0.86800E5	0.36240E4	0.34667E2			
9	0.41559E6	0.23034E5	0.38533E3			
10	0.19887E7	0.13659E6	0.34200E4	0.13000E2		
11	0.94787E7	0.78511E6	0.26309E5	0.29550E3		
12	0.45166E8	0.43674E7	0.18361E6	0.32040E4	0.10182E2	
13	0.21463E9	0.23850E8	0.12073E7	0.30024E5	0.20701E3	
14	0.10198E10	0.12784E9	0.75424E7	0.23879E6	0.29680E4	0.26667E1
15	0.48360E10	0.67687E9	0.45650E8	0.17684E7	0.32705E5	0.10133E3
(*b*)	$X^3(l, I)$					
3	0.10300E3					
4	0.74400E3	0.00000E0				
5	0.48690E4	0.60000E1				
6	0.29936E5	0.12400E3				
7	0.17620E6	0.16140E4	0.20000E1			
8	0.10049E7	0.15696E5	0.82667E2			
9	0.55945E7	0.13115E6	0.11453E4			
10	0.30563E8	0.98561E6	0.12968E5	0.13000E2		
11	0.16444E9	0.68918E7	0.12384E6	0.61050E3		
12	0.87375E9	0.45638E8	0.10627E7	0.98790E4	0.10182E2	
13	0.45942E10	0.29000E9	0.83989E7	0.11734E6	0.53864E3	
14	0.23943E11	0.17830E10	0.62300E8	0.11670E7	0.96676E4	0.10667E2
15	0.12383E12	0.10676E11	0.43943E9	0.10354E8	0.12700E6	0.27733E3
(*c*)	$X^5(l, I)$					
3	0.51100E3					
4	0.52560E4	0.00000E0				
5	0.45405E5	0.60000E1				
6	0.35074E6	0.36400E3				
7	0.25069E7	0.76140E4	0.20000E1			
8	0.16922E8	0.10526E6	0.27467E3			
9	0.10934E9	0.11533E7	0.58653E4			
10	0.68242E9	0.10868E8	0.86040E5	0.13000E2		
11	0.41418E10	0.92120E8	0.10196E7	0.18705E4		
12	0.24565E11	0.72180E9	0.10539E8	0.46719E5	0.10182E2	
13	0.14290E12	0.53231E10	0.98443E8	0.75359E6	0.18652E4	
14	0.81766E12	0.37414E11	0.85047E9	0.94785E7	0.51259E5	0.42667E2
15	0.46128E13	0.25289E12	0.68989E10	0.10223E9	0.83913E6	0.16213E4

vectors are chosen for convenience, as [15]:

$$\hat{\boldsymbol{a}}_1 = \frac{1}{\sqrt{2}}(\hat{\boldsymbol{x}} + \hat{\boldsymbol{y}}) \qquad \hat{\boldsymbol{a}}_2 = \frac{1}{\sqrt{2}}(\hat{\boldsymbol{y}} + \hat{\boldsymbol{z}}) \qquad \hat{\boldsymbol{a}}_3 = \frac{1}{\sqrt{2}}(\hat{\boldsymbol{z}} + \hat{\boldsymbol{x}}) \tag{3}$$

where the $1/\sqrt{2}$ is a normalisation factor so that each bond is of length unity. The enumeration is performed with the first monomeric site rooted at the origin and the first

step fixed along $\hat{\boldsymbol{a}}_1$. It is then easy to see that there are only four sets of topologically distinct configurations [15]:

(i) the second step is along $\hat{\boldsymbol{a}}_1$;
(ii) the second step is along $\pm\hat{\boldsymbol{a}}_1 \wedge \hat{\boldsymbol{z}}$;
(iii) the second step is either along $\hat{\boldsymbol{a}}_3$, $\hat{\boldsymbol{a}}_2$, $-\hat{\boldsymbol{a}}_3 \wedge \hat{\boldsymbol{y}}$ or $-\hat{\boldsymbol{a}}_2 \wedge \hat{\boldsymbol{x}}$; and
(iv) the second step is either along $\hat{\boldsymbol{a}}_3 \wedge \hat{\boldsymbol{y}}$, $\hat{\boldsymbol{a}}_2 \wedge \hat{\boldsymbol{x}}$, $-\hat{\boldsymbol{a}}_3$ or along $-\hat{\boldsymbol{a}}_2$,

where the $\wedge$ denotes a vector cross product. Care should be exercised to make sure that contributions (both positively and negatively) from different projected components are accounted for. Tables 3 and 4 present the first three odd moments of the persistence lengths for trails and silhouettes, respectively. The tabulations here are up to a chain length of $l = 10$ and a maximum number of intersections of $I = 5$. Hence we see that the enumerations on the simple cubic lattice and the face-centred cubic lattice are up to the same term in the expansion of equation (2) as a series in $e^{I\theta}$.

Table 3. Trails on a face-centred cubic lattice: (*a*) the first odd moment of the persistence length $X(l, I)$; (*b*) the second odd moment of the persistence length $X^3(l, I)$; (*c*) the third odd moment of the persistence length $X^5(l, I)$.

l	$I = 0$	$I = 1$	$I = 2$	$I = 3$	$I = 4$	$I = 5$
(*a*)	$X(l, I)$					
2	0.12000E2					
3	0.13300E3	0.00000E0				
4	0.14260E4	0.34000E2				
5	0.15023E5	0.94200E3	0.24000E2			
6	0.15662E6	0.17072E5	0.88400E3			
7	0.16218E7	0.25806E6	0.21862E5	0.21200E3		
8	0.16714E8	0.35335E7	0.42659E6	0.15712E5	0.11200E3	
9	0.17165E9	0.45501E8	0.71505E7	0.49856E6	0.11224E5	
10	0.17580E10	0.56207E9	0.10848E9	0.11296E8	0.50473E6	0.37520E4
(*b*)	$X^3(l, I)$					
2	0.24000E2					
3	0.42100E3	0.00000E0				
4	0.63445E4	0.35500E2				
5	0.87546E5	0.17700E4	0.15000E2			
6	0.11406E7	0.48968E5	0.14600E4			
7	0.14275E8	0.10287E7	0.53257E5	0.14900E3		
8	0.17344E9	0.18413E8	0.13762E7	0.22090E5	0.64000E2	
9	0.20597E10	0.29684E9	0.29324E8	0.10815E7	0.14188E5	
10	0.24024E11	0.44468E10	0.55059E9	0.33395E8	0.95555E6	0.42440E4
(*c*)	$X^5(l, I)$					
2	0.64500E2					
3	0.18730E4	0.00000E0				
4	0.40229E5	0.35875E2				
5	0.73122E6	0.45120E4	0.12750E2			
6	0.11942E8	0.20420E6	0.34940E4			
7	0.18102E9	0.60830E7	0.20040E6	0.13325E3		
8	0.25970E10	0.14316E9	0.70777E7	0.48494E5	0.52000E2	
9	0.35719E11	0.28928E10	0.19341E9	0.36662E7	0.27589E5	
10	0.47511E12	0.52530E11	0.44842E10	0.15647E9	0.29305E7	0.70070E4

Table 4. Silhouettes on a face-centred cubic lattice: (*a*) the first odd moment of the persistence length $X(l, I)$; (*b*) the second odd moment of the persistence length $X^3(l, I)$; (*c*) the third odd moment of the persistence length $X^5(l, I)$.

l	$I = 0$	$I = 1$	$I = 2$	$I = 3$	$I = 4$	$I = 5$
(*a*)	$X(l, I)$					
2	0.12000E2					
3	0.13300E3	0.00000E0				
4	0.14260E4	0.17000E2				
5	0.15023E5	0.47100E3	0.40000E1			
6	0.15662E6	0.85360E4	0.14733E3			
7	0.16218E7	0.12903E6	0.37613E4	0.13250E2		
8	0.16714E8	0.17667E7	0.76343E5	0.97692E3	0.25455E1	
9	0.17165E9	0.22751E8	0.13251E7	0.31148E5	0.23602E3	
10	0.17580E10	0.28103E9	0.20692E8	0.72341E6	0.10382E5	0.24764E2
(*b*)	$X^3(l, I)$					
2	0.24000E2					
3	0.42100E3	0.00000E0				
4	0.63445E4	0.17750E2				
5	0.87546E5	0.88500E3	0.25000E1			
6	0.11406E7	0.24484E5	0.24333E3			
7	0.14275E8	0.51437E6	0.90098E4	0.93125E1		
8	0.17341E9	0.92064E7	0.23903E6	0.13766E4	0.14545E1	
9	0.20597E10	0.14842E9	0.52466E7	0.67306E5	0.31075E3	
10	0.24024E11	0.22234E10	0.10136E9	0.21142E7	0.20073E5	0.29881E2
(*c*)	$X^5(l, I)$					
2	0.64500E2					
3	0.18730E4	0.00000E0				
4	0.40229E5	0.17937E2				
5	0.73122E6	0.22560E4	0.21250E1			
6	0.11942E8	0.10210E6	0.58233E3			
7	0.18102E9	0.30415E7	0.33537E5	0.83281E1		
8	0.25970E10	0.71581E8	0.12035E7	0.30272E4	0.11818E1	
9	0.35719E11	0.14464E10	0.33661E8	0.22812E6	0.61715E3	
10	0.47511E12	0.26265E11	0.80090E9	0.98475E7	0.62791E5	0.51161E2

3.3. Some inferences

From tables 1–4 and the $c(l, I)$ tables of [13–15], it is easy to see that for both the simple cubic lattice and the face-centred cubic lattice, the reduced moment

$$\bar{M}_l^{2k+1}(\theta) = \frac{\langle X_l^{2k+1}(\theta)\rangle}{\langle X_l^{2r+1}(\theta)\rangle^{(2k+1)/(2r+1)}} \geq 1 \qquad \forall\, r < k \tag{4}$$

where the equality sign holds only for $l = 1$. This behaviour has also been observed in 2D [1, 4, 15]. The inequality is a direct consequence of the faster rate of increase of the higher moments. It can also be easily verified that $\bar{M}_l^{2k+1}(\theta)$ increases as θ increases [15]. Such behaviour has also been noted in 2D [1, 17].

4. Analysis of the data

As in [1], we shall try to fit the averaged odd moments of the persistence lengths with

a scaling law of the form

$$\langle X_l^{2k+1}(\theta)\rangle = \begin{cases} A_0(\theta) f(l) & \text{if } k = 0 \\ A_k(\theta) l^{pk\nu(\theta)} f(l) & \text{if } k = 1, 2, \ldots \end{cases} \tag{5}$$

where the arguments θ show explicitly any possible temperature dependence, p is a parameter, $f(l)$ is some function of l and the $A_k(\theta)$ are the amplitudes (or prefactors). As can easily be shown (at least heuristically) [4, 5], $f(l) \sim$ constant in 3D. In order to investigate this numerically, we shall analyse the persistence lengths of trails and silhouettes by taking the Naperian logarithms of equation (5):

$$\log_{10}\langle X_l^{2k+1}(\theta)\rangle = pk\nu(\theta)\log_{10} l + \log_{10} f(l) + \log_{10} A_k(\theta). \tag{6}$$

In addition, we will also study the differences in averaged moments of persistence lengths of silhouettes and trails [1]

$$\Delta_l^{2k+1}(\theta) = \langle X_l^{2k+1}(\theta)\rangle_{\text{silh}} - \langle X_l^{2k+1}(\theta)\rangle_{\text{trail}}. \tag{7}$$

To summarise, we shall analyse on each lattice (as in [1]) the persistence lengths in three steps:

(1) the variation of persistence lengths with chain length;
(2) the temperature dependence of the persistence lengths, and
(3) the variation of $\Delta_l^{2k+1}(\theta)$ with temperature.

5. Analysis for trails and silhouettes on a simple cubic lattice

5.1. Variation with chain length

Figures 1(*a*)–1(*d*) are plots of $\log_{10}\langle X_l^{2k+1}\rangle$ against $\log_{10} l$ at two different temperatures of $\theta = 0.0$ and $\theta = 4.0$. It is very obvious that in the hot region (for example $\theta = 0.0$), the plots are linear so that we can perform a linear regression on the data in this region.

Table 5(*a*) tabulates the gradients (see equation (6)) of the log–log plots for $-5 \leq \theta \leq 5$ and table 5(*b*) gives the intercepts of the plots in the same temperature range. The regression coefficients are averages of the coefficients obtained from $l_{\min} \leq l \leq l_{\max}$ where $l_{\min} = 7, \ldots, 11$ and $l_{\max}$ is held fixed at 15. It is interesting to note that for the $k = 0$ case, the gradient $pk\nu \sim 10^{-2}$ and the intercept is a constant (~ 0.1), an observation that can be corroborated with the fact that $f(l) \sim$ constant.

5.2. Variation with temperature

Figures 2(*a*) and 2(*b*) are representative plots of the variation of the averaged persistence lengths with temperature, $\langle X^7\rangle$ against θ for $10 \leq l \leq 15$. It is seen from the plots that the averaged persistence lengths remain at a constant value for low values of θ (swollen region), and then decrease very rapidly within a relatively narrow range of θ to another constant value. As in 2D [1], it is also observed that this collapse occurs

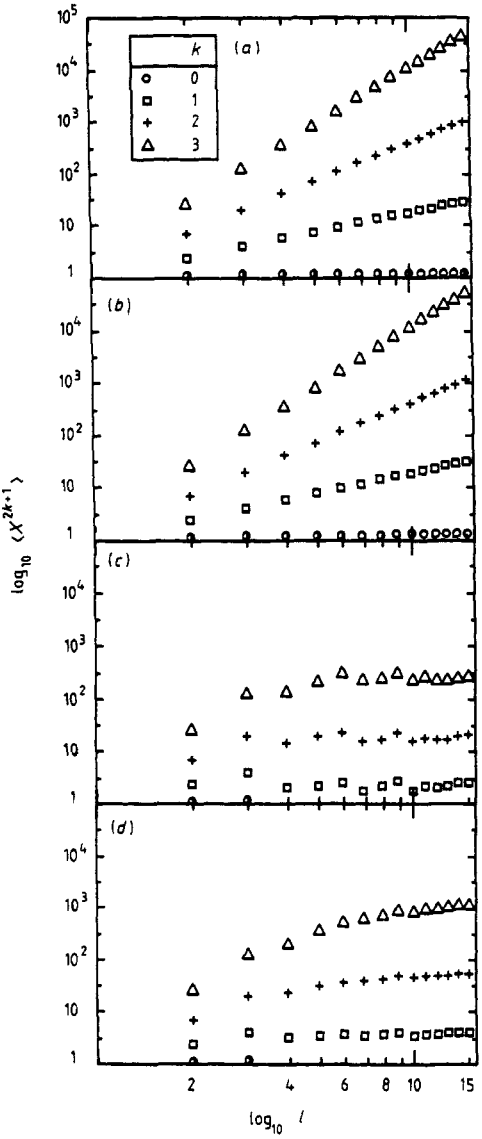

Figure 1. Log–log plots of $\langle X\rangle$, $\langle X^3\rangle$, $\langle X^5\rangle$ and $\langle X^7\rangle$ against l at a constant $\theta = 0.0$ in (a) trails and (b) silhouettes on a simple cubic lattice; at a constant $\theta = 4.0$ in (c) trails and (d) silhouettes on a simple cubic lattice.

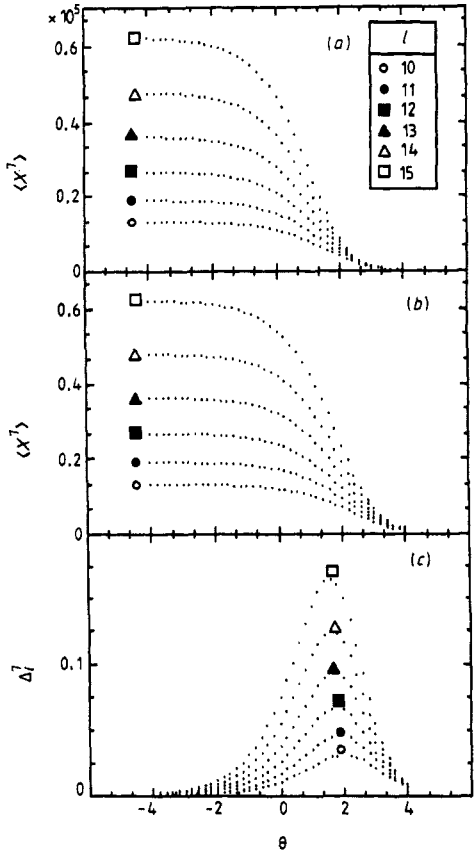

Figure 2. Plots of $\langle X^7\rangle$ against θ for $l = 10$–15 in (a) trails and (b) silhouettes on a simple cubic lattice; (c) a plot of Δ_l^7 for $l = 10$–15.

at a higher value of θ for silhouettes than that for trails. We note in particular that at $\theta = -\infty$ (SAW)

$$pkv = \begin{cases} 1.293 & \text{if } k = 1 \\ 2.555 & \text{if } k = 2 \\ 3.815 & \text{if } k = 3 \end{cases} \tag{8}$$

Table 5. The values of (*a*) the linear regression coefficients of the Naperian logarithm and (*b*) the prefactors for the first four odd moments of the persistence lengths for trails and silhouettes on a simple cubic lattice.

	Trails				Silhouettes			
θ	$k=0$	$k=1$	$k=2$	$k=3$	$k=0$	$k=1$	$k=2$	$k=3$
(*a*) *pkv*								
$-\infty$	0.034	1.293	2.555	3.815	0.034	1.293	2.555	3.815
−5.0	0.034	1.293	2.555	3.815	0.035	1.294	2.556	3.816
−4.0	0.034	1.292	2.554	3.812	0.034	1.293	2.555	3.815
−3.0	0.033	1.289	2.548	3.805	0.035	1.291	2.552	3.811
−2.0	0.032	1.280	2.532	3.785	0.033	1.287	2.545	3.801
−1.0	0.026	1.253	2.489	3.729	0.030	1.274	2.524	3.774
0.0	0.010	1.175	2.364	3.569	0.024	1.240	2.466	3.700
1.0	−0.035	0.941	1.993	3.101	0.003	1.143	2.309	3.497
2.0	−0.093	0.414	1.095	1.931	−0.044	0.891	1.899	2.969
3.0	−0.012	0.093	0.168	0.410	−0.076	0.443	1.093	1.877
4.0	0.140	0.432	0.321	0.008	0.032	0.236	0.389	0.654
5.0	0.231	0.939	1.154	0.807	0.203	0.553	0.546	0.347
(*b*) $\log_{10} A_k$								
$-\infty$	0.096	0.024	0.111	0.308	0.096	0.024	0.111	0.308
−5.0	0.096	0.024	0.111	0.308	0.096	0.024	0.110	0.307
−4.0	0.097	0.025	0.112	0.310	0.097	0.024	0.111	0.308
−3.0	0.097	0.026	0.115	0.314	0.095	0.025	0.112	0.311
−2.0	0.095	0.030	0.124	0.327	0.096	0.027	0.117	0.317
−1.0	0.095	0.042	0.150	0.364	0.095	0.032	0.129	0.335
0.0	0.092	0.082	0.228	0.473	0.093	0.048	0.163	0.383
1.0	0.093	0.220	0.478	0.808	0.091	0.096	0.259	0.519
2.0	0.064	0.539	1.104	1.673	0.085	0.231	0.522	0.883
3.0	−0.126	0.542	1.577	2.656	0.022	0.452	1.027	1.634
4.0	−0.362	−0.094	0.926	2.408	−0.192	0.353	1.283	2.316
5.0	−0.498	−0.807	−0.300	1.037	−0.442	−0.243	0.659	2.006

which, after substituting $\nu(\mathrm{SAW}) = 3/5$, yield

$$p = \begin{cases} 2.155 & \text{if } k = 1 \\ 2.129 & \text{if } k = 2 \\ 2.119 & \text{if } k = 3. \end{cases} \tag{9}$$

These results are in very good agreement with $p = 2.0$ obtained from scaling analysis [5].

5.3. *Variation of* Δ_l^{2k+1} *with temperature*

Figure 2(*c*) displays Δ_l^{2k+1} against θ for $10 \leq l \leq 15$. As θ increases from $-\infty$ to $+\infty$, Δ_l^{2k+1} increases from zero, attains a maximum and then decreases back to zero. The two tails are explained by the fact that in the swollen phase (hot region) and in the collapse phase (cold region), trails and silhouettes share a common exponent of $\nu = 3/5$ and $\nu = 1/d$ respectively (where we recall d is the dimensionality). The non-vanishing value of Δ_l^{2k+1} is a direct consequence of the fact that collapse occurs at a higher value of θ in silhouettes than in trails.

6. Analysis for trails and silhouettes on a face-centred cubic lattice

6.1. Variation with chain length

Figures 3(*a*) and 3(*b*) are plots of $\log_{10}\langle X_l^{2k+1}\rangle$ against $\log_{10} l$ for trails and silhouettes, respectively. The regression coefficients, obtained from $l_{\min} \leq l \leq l_{\max}$ where $l_{\min} = 4,\ldots,8$ and $l_{\max} = 10$, are tabulated in tables 6(*a*) and 6(*b*). Again we note here that for the $k = 0$ case, the gradient $pkv \sim 10^{-2}$ and the intercept is a constant (~ 0.04). This should be contrasted with the results in 2D where $pkv = 10^{-1}$ for the $k = 0$ case. For larger values of θ (figures 3(*c*) and 3(*d*)), the log–log plots are more erratic.

6.2. Variation with temperature

The variation of $\langle X^7\rangle$ with θ is depicted in figures 4(*a*) and 4(*b*). The qualitative behaviour is very similar to that observed on the simple cubic lattice, and the same explanation is still valid for explaining the qualitative features. From table 6(*a*), at $\theta = -\infty$ (SAW)

$$pkv = \begin{cases} 1.275 & \text{if } k = 1 \\ 2.519 & \text{if } k = 2 \\ 3.785 & \text{if } k = 3 \end{cases} \tag{10}$$

which, after making the substitution $\nu(\text{SAW}) = 3/5$, give

$$p = \begin{cases} 2.125 & \text{if } k = 1 \\ 2.099 & \text{if } k = 2 \\ 2.103 & \text{if } k = 3. \end{cases} \tag{11}$$

These results are again in excellent agreement with the scaling analysis results of $p = 2.0$ [5].

6.3. Variation of Δ_l^{2k+1} with temperature

The variation of Δ_l^{2k+1} with θ is shown in figure 4(*c*) for $5 \leq l \leq 10$. The qualitative behaviour is very similar to that seen on the simple cubic lattice and may be explained similarly.

7. Discussions and conclusion

We have systematically studied the first four odd moments of the persistence lengths of trails and silhouettes on a simple cubic lattice and on a face-centred cubic lattice. The results are tabulated according to their chain lengths and the number of intersections for the first time. This tabulation allows the temperature dependence to be introduced via the conjugate fugacity factor $e^{l\theta}$, and this renders examinable the properties of persistence lengths in various temperature regions. The results seem to augment the belief that persistence lengths (in 3D) scale according to the scaling law [4, 5, 15]

$$\langle X_l^{2k+1}(\theta)\rangle \sim l^{pkv(\theta)} \tag{12}$$

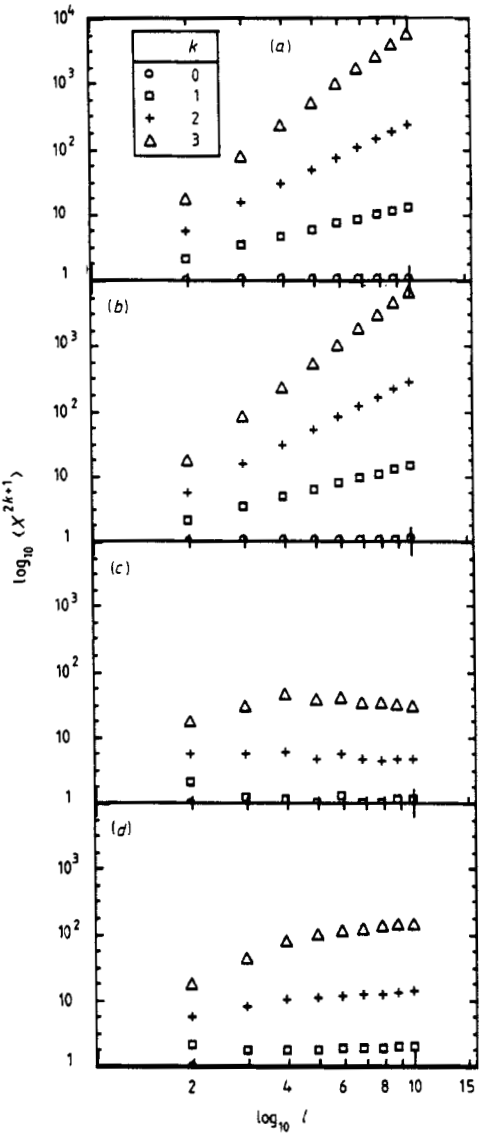

Figure 3. Log–log plots of $\langle X\rangle$, $\langle X^3\rangle$, $\langle X^5\rangle$ and $\langle X^7\rangle$ against l at a constant $\theta = 0.0$ in (*a*) trails and (*b*) silhouettes on a face-centred cubic lattice; and at a constant $\theta = 4.0$ in (*c*) trails and (*d*) silhouettes on a face-centred cubic lattice.

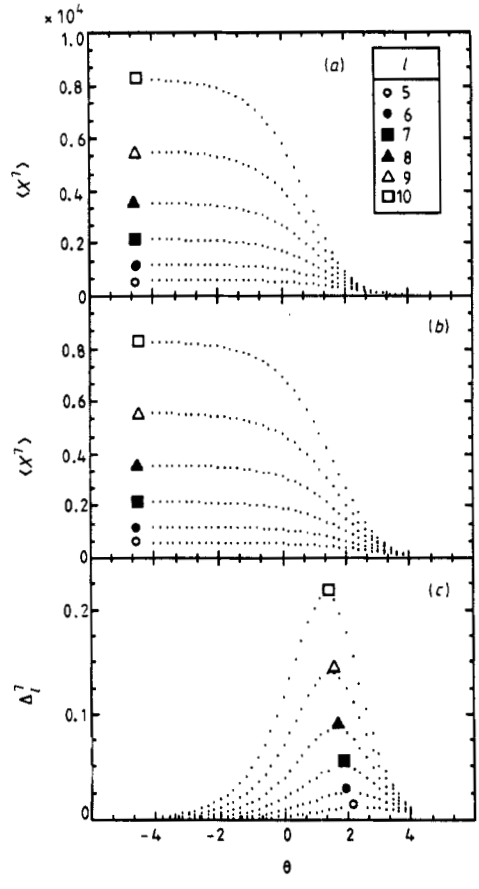

Figure 4. Plots of $\langle X^7\rangle$ against θ for $l = 5$–10 in (*a*) trails and (*b*) silhouettes on a face-centred cubic lattice; (*c*) a plot of Δ_l^7 for $l = 5$–10.

where $p = 2.0$. We have also tried to fit the enumeration data with the reduced moment [1]

$$M_l^{2k+1}(\theta) = \frac{\langle X_l^{2k+1}(\theta)\rangle}{\langle X_l(\theta)\rangle} = \frac{A_k(\theta)l^{pk\nu(\theta)}}{A_0(\theta)} \tag{13}$$

so that any possible $f(l)$ dependence may be eliminated. The linear regression coef-

Table 6. The values of (*a*) the linear regression coefficients of the Naperian logarithm and (*b*) the prefactors for the first four odd moments of the persistence lengths for trails and silhouettes on a face-centred cubic lattice.

	Trails				Silhouettes			
θ	$k=0$	$k=1$	$k=2$	$k=3$	$k=0$	$k=1$	$k=2$	$k=3$
(*a*) *pkv*								
$-\infty$	0.045	1.275	2.519	3.785	0.045	1.275	2.519	3.785
−5.0	0.043	1.274	2.517	3.783	0.043	1.274	2.518	3.784
−4.0	0.043	1.272	2.514	3.779	0.044	1.273	2.517	3.782
−3.0	0.042	1.266	2.506	3.769	0.043	1.271	2.513	3.777
−2.0	0.039	1.252	2.484	3.741	0.040	1.263	2.502	3.763
−1.0	0.031	1.211	2.421	3.663	0.037	1.244	2.471	3.726
0.0	0.008	1.097	2.245	3.445	0.027	1.192	2.390	3.624
1.0	−0.048	0.793	1.767	2.846	−0.000	1.057	2.179	3.358
2.0	−0.097	0.253	0.810	1.569	−0.048	0.762	1.692	2.730
3.0	−0.040	−0.050	−0.039	0.145	−0.059	0.356	0.912	1.628
4.0	0.049	0.117	−0.097	−0.380	0.029	0.175	0.302	0.539
5.0	0.061	0.435	0.362	−0.063	0.132	0.355	0.290	0.135
(*b*) $\log_{10} A_k$								
$-\infty$	0.042	−0.052	−0.000	0.132	0.042	−0.052	−0.000	0.132
−5.0	0.044	−0.052	0.000	0.133	0.044	−0.052	−0.000	0.133
−4.0	0.043	−0.051	0.001	0.135	0.042	−0.052	0.000	0.134
−3.0	0.043	−0.049	0.005	0.141	0.043	−0.051	0.002	0.136
−2.0	0.042	−0.043	0.016	0.156	0.044	−0.048	0.008	0.144
−1.0	0.040	−0.027	0.048	0.198	0.042	−0.040	0.022	0.164
0.0	0.037	0.024	0.140	0.320	0.038	−0.020	0.062	0.218
1.0	0.034	0.169	0.401	0.668	0.033	0.035	0.168	0.363
2.0	−0.010	0.403	0.910	1.406	0.015	0.154	0.410	0.706
3.0	−0.150	0.363	1.177	2.057	−0.064	0.267	0.752	1.269
4.0	−0.287	−0.046	0.767	1.877	−0.224	0.141	0.835	1.648
5.0	−0.326	−0.514	0.000	1.063	−0.367	−0.261	0.415	1.401

ficients obtained from this fit differ from the numbers in tables 5(*a*) and 6(*a*) only in the second decimal place. This may be taken as a sign that equation (12) provides a reasonable fit.

Quick comparisons of figures 1 and 3, especially those in the cold temperature regions, show that the averaged odd moments $\langle X_t^{2k+1}(\theta)\rangle$ are correlated. This is obvious from the defining equation (2).

Since the face-centred cubic lattice has a coordination number $q = 12$ and the simple cubic lattice has a coordination number $q = 6$, the persistence lengths in the former are expected to be lower than in the latter. This fact is clearly borne out in tables 5(*b*) and 6(*b*). It is seen that the weaker persistency on the face-centred cubic lattice is absorbed into the prefactors (see equation (5)), thus explaining the lower values of the prefactors on the face-centred cubic lattice as compared with those on the simple cubic lattice.

On each lattice, it is seen that as θ is increased, collapse occurs at a lower value of θ in trails (see figures 2(*a*) and 2(*b*), 4(*a*) and 4(*b*)). This behaviour is also very well reflected in figures 1 and 3. Closer comparison of the figures reveals that as θ is increased, the persistence lengths of silhouettes decrease, but always stay larger than or equal to those of trails. Since θ is the inverse temperature, this implies that silhouettes

collapse at a colder temperature. A plausible explanation for this behaviour is that for each silhouette, there is a multiplicity of trails and thus it is energetically more favourable for silhouettes to collapse at a colder temperature. This fact has also been observed in 2D [1].

Another noteworthy observation is that persistency is relatively weaker in 3D than in 2D [5]. This is not surprising at all since in 3D the walks have an extra physical dimension. In general, one would expect the persistency to be lower the higher the dimension, an inference in agreement with the data of [5], though not explicitly pointed out in the reference.

To summarise, we note that most of the properties of the persistence lengths observed in 2D [1] are also observed in 3D, except that $f(l) \sim \log_e l$ in 2D and $f(l) \sim$ constant in 3D. The $\log_e l$ dependence is unique of 2D. This conclusion is very reminiscent of the results of SAW [4, 5], which correspond to our $\theta \to -\infty$ limit. Since SAW are actually trails (or silhouettes) with no intersections, their persistency provides a numerical upper bound on the persistency of trails (or silhouettes).

Acknowledgments

The authors are grateful to the Technical Support Group for computing assistance during various stages of the project, Mr David V LaSalle for graphics displays, and Dr H Meirovitch for discussions. The authors also thank the Supercomputer Computations Research Institute for the use of the computer facilities. This work is partially supported by the US Department of Energy under the contract no DE-FC05-85ER250000.

References

[1] Burnette D E and Lim H A 1989 *J. Phys. A: Math. Gen.* **22** 3059
[2] Weiss G H 1981 *J. Math. Phys.* **22** 562
[3] Grassberger P 1982 *Phys. Lett.* **89A** 381
[4] Redner S and Privman V 1987 *J. Phys. A: Math. Gen.* **20** L857
[5] Considine D and Redner S 1989 *J. Phys. A: Math. Gen.* **22** 1622
[6] Noolandi J, Slater G, Lim H A and Viovy L 1989 *Science* **243** 1456
[7] Brandes R and Kearns D R 1986 *Biochem.* **25** 5890
[8] Malakis A 1975 *J. Phys. A: Math. Gen.* **8** 1885
[9] Malakis A 1976 *J. Phys. A: Math. Gen.* **9** 1283
[10] Massih A R and Moore M A 1975 *J. Phys. A: Math. Gen.* **8** 237
[11] Shapir Y and Oono Y 1984 *J. Phys. A: Math. Gen.* **17** L39
[12] Lim H A, Guha A and Shapir Y 1988 *J. Phys. A: Math. Gen.* **21** 773
[13] Guha A, Lim H A and Shapir Y 1988 *J. Phys. A: Math. Gen.* **21** 1043
[14] Lim H A, Guha A and Shapir Y 1988 *Phys. Rev.* A **38** 3710
[15] Lim H A 1988 *J. Phys. A: Math. Gen.* **21** 3783
[16] Meirovitch H and Lim H A 1988 *Phys. Rev.* A **38** 1670
[17] Rapaport D C 1977 *J. Phys. A: Math. Gen.* **10** 637